Microstructure and electrochemical properties of nitrogen-doped DLC films deposited by PECVD technique

Kai Zhou [a,b], Peiling Ke [b], Xiaowei Li [b], Yousheng Zou [a,*], Aiying Wang [b,**]

[a] School of Materials Science and Engineering, Institute of Optoelectronics & Nanomaterials, Nanjing University of Science and Technology, Nanjing, Jiangsu, 210094, PR China
[b] Key Laboratory of Marine Materials and Related Technologies, Zhejiang Key Laboratory of Marine Materials and Protective Technologies, Ningbo Institute of Materials Technology & Engineering, Chinese Academy of Sciences, Ningbo, 315201, PR China

ARTICLE INFO

Keywords:
Nitrogen-doped diamond-like carbon
Bias voltage
Microstructure
Electrochemical properties

ABSTRACT

Nitrogen-doped diamond-like carbon (N-DLC) films were synthesized by glow discharge plasma enhanced chemical vapor deposition (PECVD) using a hybrid ion beam system. The influence of nitrogen incorporation on the microstructure and electrochemical properties of N-DLC films was investigated by scanning probe microscopy, Raman spectroscopy, X-ray photoemission spectroscopy and cycle voltammetry. Regardless of the deposition parameters, the surface of all the deposited films is very smooth. Raman spectra show that I_D/I_G increases from 0.6 to 1.04 with the substrate bias voltage increases. XPS results identify that carbon is bonded with nitrogen and the substrate bias makes no distinct contribution to the N content in the films, even the N-DLC film at bias of −550 V has the lowest N–O bonds concentration and the highest C–N bonds concentration. The film electrodes show the wide potential windows range over 4 V, lower background currents in strong acid media. At the bias of −550 V, the N-DLC film electrode not only exhibits the ΔE_p at 209 mV and I_p^{ox}/I_p^{red} at 0.8778 in $K_3Fe(CN)_6$ solution, respectively, but also illustrates a nearly reversible electrode reaction. The mechanism of electroproperties is discussed in terms of the atomic bond structures and diffusion process.

1. Introduction

The unique properties of highly boron-doped diamond (BDD) electrodes, including anti-toxic, good corrosion resistance, a wide potential window and a low background current, have made them successfully apply to the detection of heavy metal [1,2] and organic compound [3,4]. The application of BDD as electrode materials also has been investigated intensely [5–8]. However, some practical problems, such as high substrate temperature of about 800 °C [9] and difficulty in controlling the deposition parameter for diamond deposition limited the applications of diamond films. Nowadays, diamond-like carbon (DLC) film, one family of amorphous carbon materials, is considered as an attractive carbon electrode material showing similar potential windows with respect to the aqueous solvent stability and a good electrochemical reactivity [10], and is also believed to be an inexpensive and potential alternative to BDD electrode. Generally, DLC films are composed of C-sp^2 and C-sp^3 atomic bonds, which make them the superior properties such as high hardness, low friction coefficient, high electrical resistivity, good chemical inertness and biocompatibility. So far, DLC films, as protective coatings, have been widely used in the fields of magnetic storage media [11], cutting tools [12], implants in human body [13], etc.

The properties of DLC can be changed by addition of other elements. The high ohmic resistivity of DLC could be significantly decreased by using doping. Previous reports have demonstrated that third element doping using various dopants, such as B, N, Zn, P and I, can improve the electrical conductivity [14–18]. The doped N atom into DLC film can raise the Fermi level towards the conduction band and narrow the band gap by graphitization of the bonding structure, which resulted in the enhancement of the conductivity of DLC films [19,20]. As such, nitrogen doped DLC (N-DLC) with wide potential window, low double layer capacitance and low background current has recently attracted attention and could be used for electrode materials [21–24]. Furthermore, in contrast to that of diamond films, the N-DLC film with the atomically smooth surface can be deposited on virtually any substrate at ambient temperature. N-DLC or nitrogen-doped ta-C film electrode with

* Corresponding author. Tel.: +86 25 84313349; fax: +86 25 84315159.
** Corresponding author. Fax: +86 574 86685159.
E-mail addresses: yshzou75@gmail.com (Y. Zou), aywang@nimte.ac.cn (A. Wang).

prominently improved electrical and electrochemical properties had the desired voltammetric characteristics suitable for electrochemical analysis or water treatment [10,25–28]. Sopchak et al. [29] studied the detection of dopamine and ascorbate with N-DLC electrodes, and demonstrated the improved sensitivity and linear dynamic range. Liu and Liu [30] reported that the N-DLC electrodes were sensitive to metal ions (Cu^+, Pb^+) in aqueous solutions. In addition, Yang et al. [31] showed that N-DLC films without conventional pretreatment were characterized by a low background voltammetric current, a wide working potential window (~3 V), and relatively rapid electron-transfer kinetics for aqueous redox systems, including $Fe(CN)_6^{-3/-4}$ and $Ru(NH_3)_6^{+3/+2}$. Even with these published works, it is still necessary to develop an electrode with much larger working potential window and a reversible electrode reaction for further electrochemical applications.

In this work, we developed the traditional glow discharge plasma enhanced chemical vapor deposition (PECVD) technique to fabricate the N-DLC films with large, electroactive surface area as well as the advantage of simple process, low deposition temperature and cost. The structural characteristics and electrode activities as well as the influence of N atoms concentration on electrochemical properties of the deposited N-DLC films were investigated. It was found that a large working potential window ~4 V and a nearly reversible electrode reaction of $K_3Fe(CN)_6$ were achieved for the N-DLC films without complex deposition technique and further plasma surface modification treatment.

2. Experimental details

N-DLC films were deposited on highly doped n-Si (the resistivity was 0.001~0.005 Ω cm) substrates by glow discharge PECVD using a hybrid ion beam system. The substrates were cleaned ultrasonically in acetone for 15 min and dried in air before they were loaded into the vacuum chamber. Prior to deposition, the chamber was firstly evacuated below 2.0×10^{-5} Torr, and then the silicon substrates were sputter-cleaned for 6 min using Ar ions with a substrate bias voltage of −100 V. During the deposition, C_2H_2 gas with a flow rate of 40 sccm and N_2 gas with a flow rate of 60 sccm were introduced into the vacuum chamber. The work pressure was kept at about 7 mTorr through a pressure throttle control valve. N-DLC films were prepared under different substrate bias voltage varying from −300 to −550 V. The thickness of the deposited N-DLC films was maintained at about 110~130 nm by controlling the deposition time.

A surface profilometer (Alpha-step IQ, US) was used to measure the thicknesses of the deposited films. Raman spectroscopy (RenishawinVia-reflex) equipped with a He–Ne laser of 532 nm exciting wavelength was used to evaluate the carbon atomic bond structure in the films. The composition and chemical bonds of the N-DLC films were analyzed by XPS (Axis ultraDLD) with Al (mono) K_α irradiation at a pass energy of 160 eV. Before commencing the measurement, an Ar^+ ion beam with an energy of 2 keV was used to etch the sample surface for 5 min to remove any contaminants. The relative N/C atomic ratio of the films was determined based on the atomic sensitivity factors and area ratio of the C1s to N1s peaks in XPS spectra of the films. The morphologies of N-DLC films were characterized by using scanning probe microscopy (SPM, Dimension 3100).

The electrochemical experiments were carried out in a Solartron 1400 multi-channel electrochemical test system at room temperature using Ag/AgCl as a reference electrode and platinum foil as a counter electrode. The prepared N-DLC films were used as a working electrode, and the edges and backsides of N-DLC films were sealed by epoxy resin with the apparent geometric surface area of 0.2~0.3 cm^2. The electrochemical potential windows were measured in 0.5 M H_2SO_4 solution and 0.1 M NaOH solution at a scan rate of 50 mV s^{-1}, respectively. The electrochemical kinetics of the $Fe(CN)_6^{4-}/Fe(CN)_6^{3-}$ redox reaction on the N-DLC film was investigated in an unstirred 10 mM $K_3Fe(CN)_6$/1 M KCl solution. The potential was scanned from 0.2 to 0.8 V with different scan rates of 20, 50, 80, 110, 140, 170 and 200 mV s^{-1}. All the chemicals employed in the present study were analytical reagent grades.

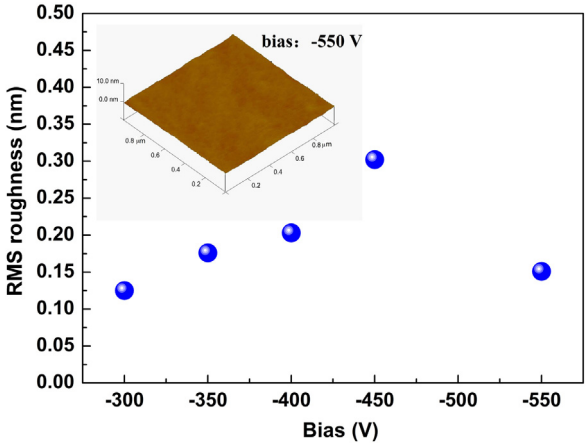

Fig. 1. RMS roughness of N-DLC films deposited at different bias voltages, inset shows the surface morphology of film at bias of −550 V.

3. Results and discussion

3.1. Growth and surface morphologies

The measurement result of surface profilometer shows that the deposition rate of the films increased monotonously from 0.9 to 3.7 nm/min by increasing the bias voltage from −300 to −550 V. This is due to the increased density of ions decomposed by the high kinetic energy.

Since the electrochemical performance of electrode materials is closely related to the surface morphology of deposited films, atomic force microscope was employed to characterize the morphological features of the deposited N-DLC films. The results show that all the deposited N-DLC films in Fig. 1 display the smooth surface similar to that of typical pure amorphous DLC films. While increasing the substrate bias from −300 V to −350 V, −400 V, −450 and −550 V, the root-mean-square surface roughness (σ_{rms}) of the deposited N-DLC films is about 0.125, 0.176, 0.203, 0.302 and 0.151 nm, respectively. Noticeably that less than bias of −350 V or higher than bias of −550 V, the σ_{rms} values of the deposited films are smaller, corresponding to the smoother surface. As reported [31], both the promoted clustering of nitrogen in the DLC films and the effect of ion bombardment with high energy could contribute to the σ_{rms} evolution of the deposited N-DLC films.

3.2. Microstructure characterization and composition

Fig. 2(a) shows the visible Raman spectra of the N-DLC films deposited at different bias voltages. All the spectra displays two obvious peaks, the first-order peak of carbon in the range of 800~1800 cm^{-1} centered at about 1500 cm^{-1} representing feature of amorphous hydrogenated DLC films (a-C:H), and the second-order peak of silicon centered at about 960 cm^{-1} caused by the opaque feature of thinner films. Generally, the first-order peaks of carbon showing broad asymmetric band can be deconvolved into two Gaussian peaks: G peak around 1560 cm^{-1} and D peak around 1350 cm^{-1}, typical for a-C:H films, where the G band is assigned to the sp^2 stretching mode of aromatic ring (corresponding to the

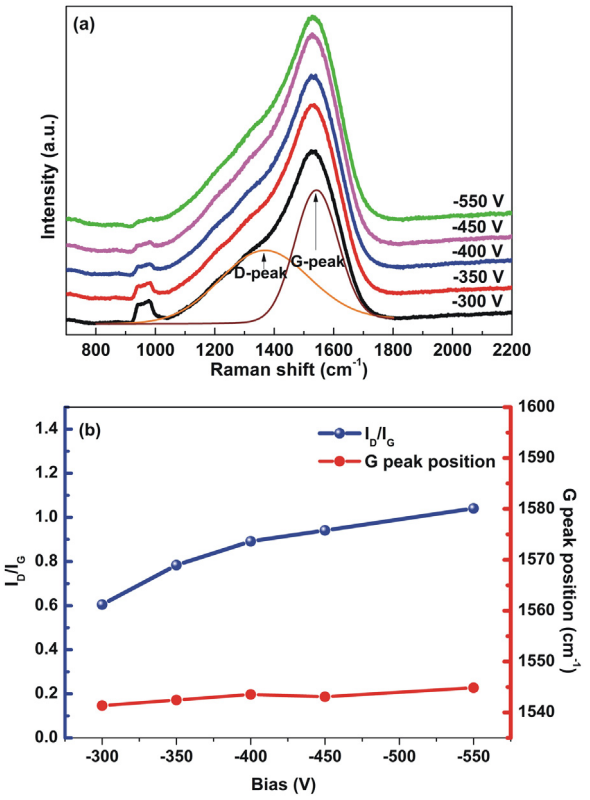

Fig. 2. (a) Raman spectra of N-DLC films deposited at different bias voltages, (b) I_D/I_G intensity ratio and G peaks positions obtained from Raman spectra of deposited N-DLC films.

optical E_{2g} phonons at the Brillouin zone center) and is present in all sp^2-bond carbons, while the D band is attributed to the breathing motion of six-fold aromatic in amorphous carbon (corresponding to the transverse optical phonons near the K point) [32]. Thereafter, the atomic bond structure of DLC films can be acquired from the G peak position, D peak position, and the intensity ratio of D peak to G peak (I_D/I_G) [33,34].

By deconvoluting the Raman spectra into G and D peak with a Gaussian fitting [35,36], the I_D/I_G ratio and G peak position of the N-DLC films deposited at various bias voltages are shown in Fig. 2(b). As the bias increased from −300 V to −550 V, the G peak position shifts upwards slightly from 1541 to 1544 cm^{-1} due to the small amount of doped N introduction effect in DLC matrix, while a significant increase in I_D/I_G from 0.6 to 1.04 is observed, indicating the increases of vibrating modes in the D band of N-DLC films and the sp^2 clusters size with increasing the bias voltage.

To further gain insight into the atomic bond evolution, the chemical composition and chemical bonding of N-DLC films were investigated by XPS. The result of XPS shows that N content decreases slightly from 5.13% to 4.75% when the bias voltage increases from −300 V to −450 V, and then keeps constant beyond of the bias to −550 V. The results indicate that the N content in the deposited films shows slight upon the applied bias voltage in the range of −300 V to −550 V. As one example, Fig. 3 shows the XPS spectra of N-DLC film deposited at bias of −550 V before and after Ar^+ ions etching, in which the peak positions located at 284.9, 399.35 and 532.35 eV are assigned to C1s, N1s and O1s peak, respectively. After Ar^+ ions etching, the O1s peak disappears from the spectra. The existence of trace amounts of oxygen before etching could be the consequence from the small amount of oxygen absorbed in the film surface, while it was exposed in the air.

In order to identify the bonding state of the N-DLC films, the C1s and N1s peaks from XPS spectra are further analyzed by fitting

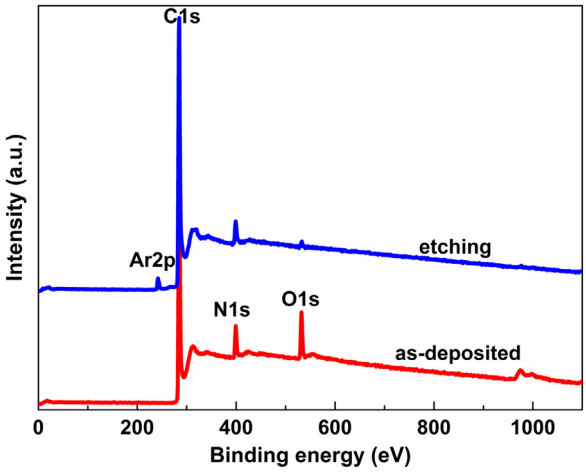

Fig. 3. XPS spectrum of N-DLC film deposited at bias voltage of −550 V.

lines at different bias voltages. Using Voigt function fitting after the inelastic background subtraction, the C1s spectra are deconvolved into four sub-peaks corresponding to different bonding state of C atoms in Fig. 4(a). Generally, the peaks at binding energy of about 284.5 eV and 285.3 eV are assigned to the sp^2C–C and sp^3C–C, respectively. While the peak at about 286.2 eV is attributed to the C–O bonding due to the sample exposure to the air. The fourth peak located at about 287.3 eV is generally assigned to the C–N bonding [37]. Fig. 4(b) shows the deconvoluted XPS N1s spectra of the films

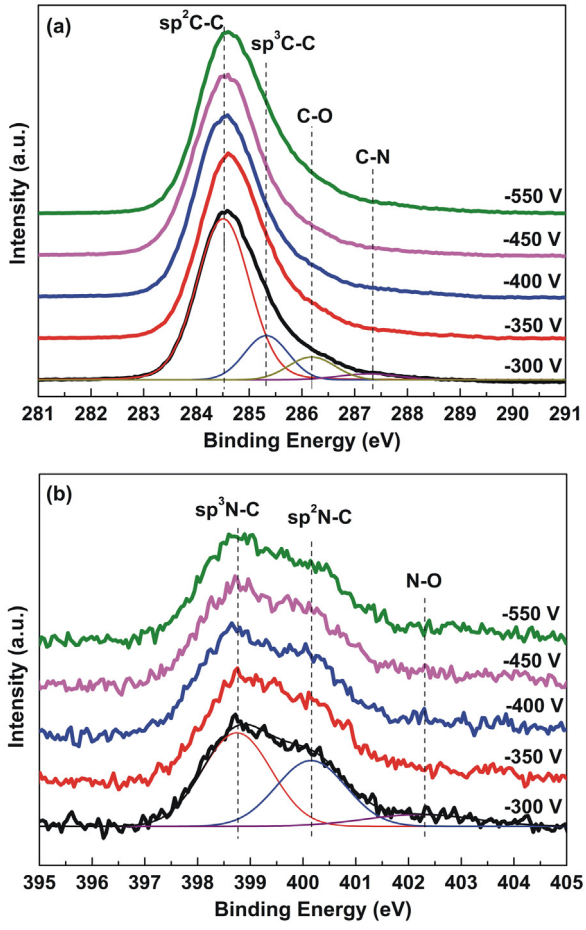

Fig. 4. Deconvolved XPS spectra of (a) C1s peaks and (b) N1s peaks for the N-DLC film at different substrate bias voltages.

deposited at various substrate bias voltages. The N1s spectra are broad and asymmetric at the higher binding energy corresponding to the several bonding configurations related to N atoms. Also the N1s spectra were deconvoluted into three peaks. The peak located at about 398.6 ± 0.1 eV and 400.1 ± 0.1 eV are corresponding to N atoms bonded to sp^3-coordinated C atoms (N-sp^3C) and N atoms bonded to sp^2-coordinated C atoms (N-sp^2C), respectively. The peak at 402.1 ± 0.2 eV is assigned to N–O bond, which is related to incorporation of oxygen into the sample due to exposure to the atmosphere. Based on the assignment and deconvolution of various carbon and nitrogen bonding states, as increasing the substrate bias from −300 V, −350 V, −400 V, −450 V and −550 V, the ratio of C-sp^2/C-sp^3 is estimated at 4.62, 4.26, 5.35, 6.48, and 5.74, respectively. This agrees quite well with the tendency of above Raman results. Meanwhile, the N–O bonding content acquired from the N1s spectra firstly increases from 10.5% to 21.8% as the bias increases from −300 V to −450 V, and then abruptly decreases to 8.56% at the bias of −550 V. Compared to the N–O bond changes, however, the C–N bonding content firstly decreases from 3.1% to 2.2% and follows by a significant increase with the increase of substrate bias voltage, and the maximum value of C–N bond content is 5.4% at bias of −550 V by calculating the bonding content. This indicates that it is not conducive to the formation of C–N bonding at bias of −450 V, and there should be more nitrogen atoms bonded with oxygen atoms during the deposition.

3.3. Electrochemical behaviors

One of the most important criteria for outstanding electrochemical properties of the electrode material is the wide potential window. The wider the potential window is, the more the elements in the solutions can be detected for heavy metal tracing analysis. So, in order to characterize the fundamental electrochemical properties of N-DLC films, the reactivity to hydrogen and oxygen evolution was investigated. Fig. 5(a) shows the cyclic voltammograms of N-DLC film electrodes deposited at different bias voltage in 0.5 M H_2SO_4 electrolyte. It demonstrates that the electrochemical potential window (ΔE) of all the N-DLC film electrodes except −450 V are estimated to be about 4.0 V, which is much higher than those reported by the others [38–41]. In addition, the redox current for N-DLC film electrode deposited at bias of −550 V is significantly higher than that for the other N-DLC films electrode. It is likely to be explained that N-DLC film (−550 V) acquires the most favorable electrochemical activation with a least amount of inactive N–O bonds that will slow down the electron transfer for the redox reaction and a most amount of active C–N bonds by XPS measurement results, which significantly raises the current respond.

Representatively, the N-DLC film electrode deposited at bias of −550 V is used to further investigate the electrochemical potential window in different solutions in order to explore its electrochemical evolution. Fig. 5(b) shows the cyclic voltammograms of N-DLC film electrode deposited at bias of −550 V in 0.5 M H_2SO_4 and 0.1 M NaOH solution at the scan rate of 50 mV s^{-1}. It can be seen that the hydrogen evolution potential and oxygen evolution potential shift to the lower potentials to some extent in NaOH solution. This implies that the potential window of the N-DLC film electrode is closely dependent on the electrolyte. The N-DLC film electrode tested in the H_2SO_4 solution exhibits a higher potential window of approximately 4.01 V compared to approximately 2.91 V measured in the NaOH solution. Moreover, the oxygen evolution potential of the N-DLC film electrode in the solution containing higher concentration of H^+ ions is higher (approximately 2.1 eV), compared to those of the film electrode in the solution containing a higher concentration of OH^- (approximately 0.88 eV). Therefore, it could be said that the N-DLC film electrodes in acidic solutions would be easier for analysis of electrochemical active species with higher

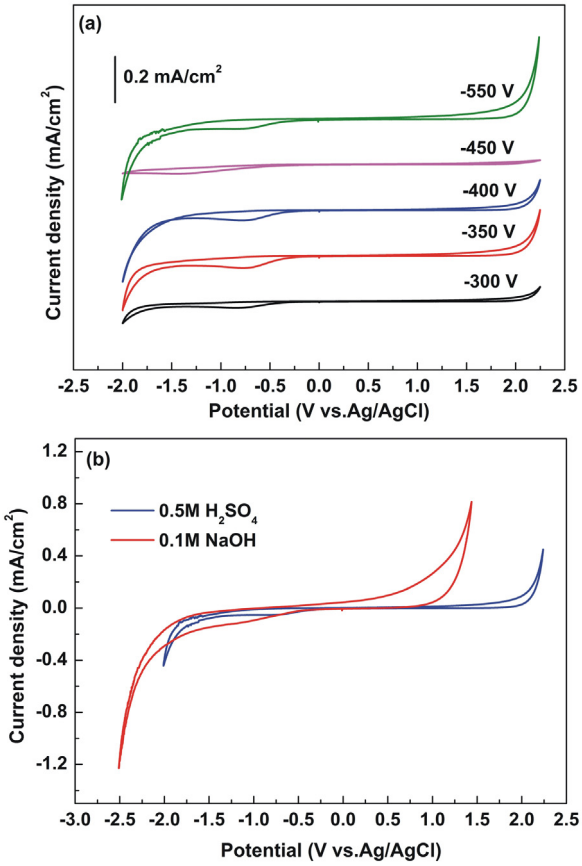

Fig. 5. (a) Cyclic voltammograms of N-DLC film electrodes deposited at different negative substrate biases in 0.5 mol L^{-1} H_2SO_4 solution and (b) N-DLC film electrode deposited at −550 V in 0.5 M H_2SO_4 solution and 0.1 M NaOH solution with a scan rate of 50 mV s^{-1}.

oxidation potential. Due to the charging effect of electrical double-layer capacitance, the background current can be observed on both the cyclic voltammograms of the N-DLC film electrodes measured in H_2SO_4 and NaOH solutions, while it was relatively smaller in acidic solution. Khun et al. [39] explained that, near the electrode, the OH^- ions ionized from NaOH were easier reacted with the hydronium ions to form the water molecules. This kind of water layer was adsorbed on the film electrode surface and the ions were surrounded by the water hydration sheath, causing the separation of the charges. Therefore, the cyclic voltammograms of the N-DLC film electrodes measured in the hydroxide solutions shows the higher background current.

The electrochemical behavior of the N-DLC film electrode was evaluated by the analysis of redox couples of $Fe(CN)_6^{3-/4-}$. Fig. 6 shows the cyclic voltammograms of 0.01 M $K_3Fe(CN)_6$ in 1 M KCl solution at the scan rate of 50 mV s^{-1} on N-DLC film electrodes deposited at various negative substrate biases. Well-defined and symmetric CV curves of $[Fe(CN)_6]^{3-}/[Fe(CN)_6]^{4-}$ on the N-DLC films electrode are obtained with the exception of bias at −450 V. The anodic peak potential to cathodic peak potential separations (ΔE_p) and the ratio of anodic and cathodic peak currents (I_p^{ox}/I_p^{red}) for the N-DLC film electrodes are summarized in Table 1. It could be seen that ΔE_p and I_p^{ox}/I_p^{red} of N-DLC film electrode deposited at −550 V are 209 mV and 0.8778, respectively, which is closer to the theoretical value. The results suggest that there is a nearly reversible electrode reaction of $K_3Fe(CN)_6$ on the surface of N-DLC film electrode deposited at −550 V in comparsion with those of the other N-DLC film electrodes.

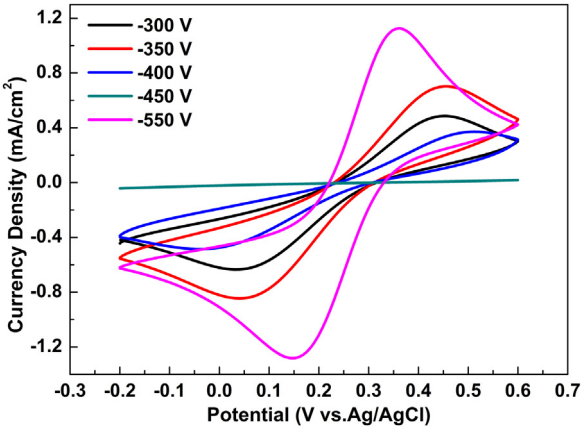

Fig. 6. Cyclic voltammograms of N-DLC film electrodes deposited at different negative substrate biases in 0.01 M $K_3Fe(CN)_6$ and 1 M KCl solution with a scan rate of 50 mV s^{-1}.

Table 1
The peak-potential separation (ΔE_p) and the ratio of anodic and cathodic peak currents (I_p^{ox}/I_p^{red}) for N-DLC film electrodes.

Bias voltage	−300 V	−350 V	−400 V	−450 V	−550 V
ΔE_p/mV	417	412	545	–	209
I_p^{ox}/I_p^{red}	0.7907	0.8298	0.7628	–	0.8778

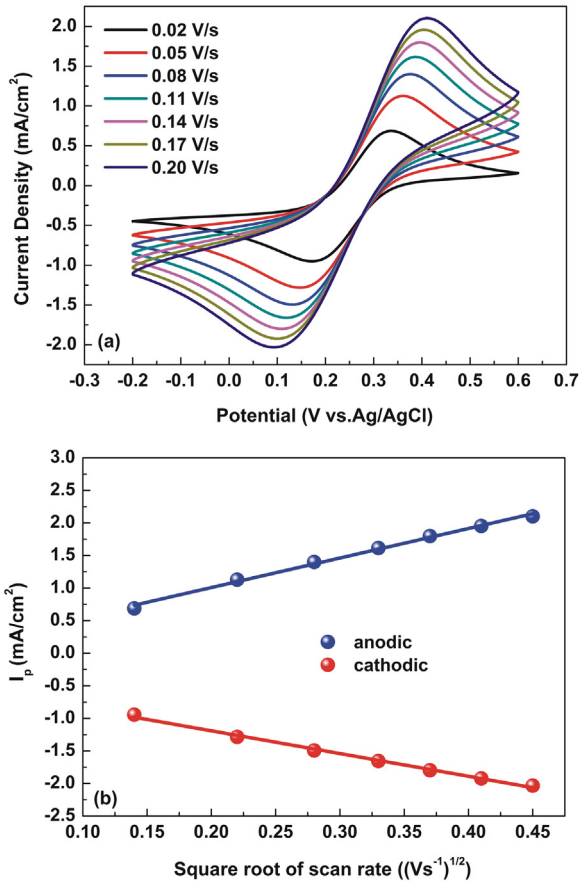

Fig. 7. (a) Cyclic voltammograms of N-DLC film electrode deposited at −550 V in 0.01 M $K_3Fe(CN)_6$ + 1 M KCl solution at various scan rates; (b) dependence of peak current densities of anodic and cathodic reactions on square root of scan rate of N-DLC film electrode at −550 V.

Fig. 7(a) shows the cyclic voltammograms of $Fe(CN)_6^{3-}/Fe(CN)_6^{4-}$ redox reaction on the N-DLC film electrode (−550 V) at various scan rates. It is found that ΔE_p values increase from 161 mV to 317 mV, and the peak current of cathodic and anodic increases with the scan rates increases from 20 to 200 mV s^{-1}. It can be explained as the effect of the increased kinetic limitation to shifting an oxidation to more positive potentials and a reduction to more negative potentials. As the scan rate increased, the experiment time scale became smaller, so that an equilibrium potential could not be reached at the film electrode surface. Fig. 7(b) shows the relation between the redox peak currents and the square root of the scan rate for the N-DLC film electrode (bias at −550 V). The electrochemical response of $Fe(CN)_6^{3-/4-}$ on the surface of N-DLC film electrode exhibits a linear relationship between the anodic or cathode peak current and square root of scan rate from 20 to 200 mV s^{-1}, as shown in Fig. 7(b), indicating a typical diffusion controlled process of the electrode reaction of $K_3Fe(CN)_6$.

4. Conclusions

N-DLC films were synthesized by the glow discharge PECVD method with a traditional pulsed DC power supply. The influence of nitrogen incorporation on the microstructure and electrochemical properties of the DLC films was investigated. The surface morphology of all the films in this study is very smooth. I_D/I_G increases from 0.6 to 1.04 with the bias voltage increases from −300 V to −550 V. XPS results identify that carbon is bonded with doped nitrogen and the substrate bias voltage almost makes no contribution to the N content changes in the films. However, N-DLC film at bias of −550 V demonstrates the lowest N–O bonds which slow down the electron transfer for the redox reaction and the highest C–N bonds contents which significantly raise the current respond. As a result, the N-DLC film electrode exhibits the wide potential windows range over 4 V, lower background currents in the strong acid media. Moreover, noted that the potential window of N-DLC electrode (bias at −550 V) is 2.91 V in alkaline solutions. This result implies that the N-DLC film electrodes in acidic solutions would be more suitable for analysis of electrochemical active species. The redox current for N-DLC film electrode deposited at bias of −550 V is significantly higher than that for the other N-DLC films electrode. Well-defined and symmetric CV curves of $[Fe(CN)_6]^{3-}/[Fe(CN)_6]^{4-}$ on the N-DLC films electrode are obtained with the exception of −450 V. The ΔE_p and I_p^{ox}/I_p^{red} of N-DLC film electrode deposited at bias of −550 V are 209 mV and 0.8778, respectively. In addition, the film electrode at −550 V shows a nearly reversible electrode reaction of $K_3Fe(CN)_6$ which is supposed to be controlled by the diffusion process. The present work provides one of the alternative promising strategies to fabricate the DLC electrodes with high performance, large area and low cost process for the electrochemical applications.

Acknowledgments

This work was financially supported by the State Key Project of Fundamental Research of China (2013CB632302, 2012CB933003), Natural Science Foundation of Jiangsu Province of China (BK20141401) and Fundamental Research Funds for the Central Universities (No.30920130111019).

References

[1] A. Sbartai, P. Namour, A. Errachid, J. Krejci, R. Sejnohova, L. Renaud, M.L. Hamlaoui, A.S. Loir, F. Garrelie, C. Donnet, H. Soder, E. Audouard, J. Granier, N. Jaffrezic-Renault, Electrochemical boron-doped diamond film microcells micromachined with femtosecond laser: application to the determination of water framework directive metals, Anal. Chem. 84 (2012) 4805–4811.

[2] J.H. Yoon, J.E. Yang, J.P. Kim, B. Kor, Simultaneous detection of Cd (II), Pb (II), Cu (II), and Hg (II) ions in dye waste water using a boron doped diamond electrode with DPASV, Chem. Soc. 31 (2010) 140–145.
[3] X. Zhu, J. Ni, J. Wei, X. Xing, H. Li, Destination of organic pollutants during electrochemical oxidation of biologically-pretreated dye wastewater using boron-doped diamond anode, J. Hazard. Mater. 189 (2011) 127–133.
[4] P.M. Natishan, W.E. O'Grady, F.J. Martin, P.L. Hagans, H. Martin, B.R. Stoner, Electrochemical oxidation of organic compounds using boron-doped diamond electrodes, ECS Trans. 45 (2013) 19–30.
[5] K.E. Toghill, R.G. Compton, Metal nanoparticle modified boron doped diamond electrodes for use in electroanalysis, Electroanal. 22 (2010) 1947–1956.
[6] S. Fierro, N. Mitani, C. Comninellis, Y. Einaga, pH sensing using boron doped diamond electrodes, Phys. Chem. Chem. Phys. 13 (2011) 16795–16799.
[7] J. Achard, F. Silva, R. Issaoui, O. Brinza, A. Tallaire, H. Schneider, K. Isoird, H. Ding, S. Kone, Thick boron doped diamond single crystals for high power electronics, Diam. Relat. Mater. 20 (2011) 145–152.
[8] D. Meziane, A. Barras, A. Kromka, J. Houdkova, R. Boukherroub, S. Szunerits, Thiol-yne reaction on boron-doped diamond electrodes: application for the electrochemical detection of DNA-DNA hybridization events, Anal. Chem. 84 (2011) 194–200.
[9] N. Mizuochi, M. Ogura, H. Watanabe, J. Isoya, H. Okushi, S. Yamasaki, EPR study of hydrogen-related defects in boron-doped p-type CVD homoepitaxial diamond films, Diam. Relat. Mater. 13 (2004) 2096–2099.
[10] K.S. Yoo, B. Miller, R. Kalish, X. Shi, Electrodes of nitrogen-incorporated tetrahedral amorphous carbon – a novel thin-film electrocatalytic material with diamond-like stability, Electrochem. Solid State Lett. 2 (1999) 233–235.
[11] J. Robertson, Diamond-like amorphous carbon, Mater. Sci. Eng. 37 (2002) 129–281.
[12] H.Y. Ueng, C.T. Guo, Diamond-like carbon coatings on microdrill using an ECR-CVD system, Appl. Surf. Sci. 249 (2005) 246–256.
[13] P. Yang, N. Huang, Y.X. Leng, J.Y. Chen, Activation of platelets adhered on amorphous hydrogenated carbon (ta-C:H) films synthesized by plasma immersion ion implantation-deposition(PIII-D), Biomaterials 24 (2003) 2821–2829.
[14] H. Naragino, K. Yoshinaga, S. Tatsuta, K. Honda, By plasma CVD methods and its electrochemical properties atoms in hydrogenated amorphous carbon films fabricated improvement of conductivity by incorporation of boron, ECS Trans. 41 (2012) 59–68.
[15] S. Liu, G.F. Wang, Z.H. Wang, Study of the conductivity of nitrogen doped tetrahedral amorphous carbon films, J. Non-Cryst. Solids 353 (2007) 2796–2798.
[16] H. Wong, Y.M. Foong, D.H.C. Chua, Improving the conductivity of diamond-like carbon films with zinc doping and its material properties, Appl. Surf. Sci. 257 (2011) 9616–9620.
[17] A.P. Liu, J.Q. Zhu, J.C. Han, H.P. Wu, W. Gao, Influence of phosphorus doping level and acid pretreatment on the voltammetric behavior of phosphorus incorporated tetrahedral amorphous carbon film electrodes, Electroanal. 17 (2007) 1773–1778.
[18] M.M. Ashraf, S. Omer, S. Adhikari, M. Adhikary, H. Rusop, T. Uchida, M. Soga, Umeno, Electrical conductivity improvement by iodine doping for diamond-like carbon thin-films deposited by microwave surface wave plasma CVD, Diam. Relat. Mater. 15 (2006) 645–648.
[19] H.L. Bai, E.Y. Jiang, Improvement of the thermal stability of amorphous carbon films by incorporation of nitrogen, Thin Solid Films 353 (1999) 157–165.
[20] A. Zeng, E. Liu, S.N. Tan, S. Zhang, J. Gao, Cyclic voltammetry studies of sputtered nitrogen doped diamond-like carbon film electrodes, Electroanal. 14 (2002) 1110–1115.
[21] A. Zeng, M.M.M. Bilek, D.R. McKenzie, P.A. Lay, Semiconductor properties and redox responses at a-C:N thin film electrochemical electrodes, Diam. Relat. Mater. 18 (2009) 1211–1217.
[22] A. Lagrini, C. Deslouis, H. Cachet, M. Benlahsen, S. Charvet, Elaboration and electrochemical characterization of nitrogenated amorphous carbon films, Electrochem. Commun. 6 (2004) 245–248.
[23] P. Tamiasso-Martinhon, H. Cachet, C. Debiemme-Chouvy, C. Deslouis, Thin films of amorphous nitrogenated carbon a-CNx: electron transfer and surface reactivity, Electrochim. Acta 53 (2008) 5752–5759.
[24] Y.V. Pleskov, M.D. Krotova, V.I. Polyakov, A.V. Khomich, A.I. Rukovishnikov, B.L. Druz, I. Zaritskiy, Electrochemical behaviour of a-C:N:H films, Electroanal. Chem. 519 (2002) 60–64.
[25] A. Zeng, E. Liu, S.N. Tan, S. Zhang, J. Gao, Stripping voltammetric analysis of heavy metals at nitrogen doped diamond-like carbon film electrodes, Electroanal. 14 (2002) 1294–1298.
[26] H. Cachet, C. Deslouis, M. Chouiki, B. Saidani, N.M.J. Conway, C. Godet, Electrochemistry of nitrogen-incorporated hydrogenated amorphous carbon films, J. Electrochem. Soc. 149 (2002) 233–241.
[27] R. McCann, S.S. Roy, P. Papakonstantinou, I. Ahmad, P. Maguire, J.A. McLaughlin, L. Petaccia, S. Lizzit, A. Goldoni, NEXAFS study and electrical properties of nitrogen-incorporated tetrahedral amorphous carbon films, Diam. Relat. Mater. 14 (2005) 1057–1061.
[28] A. Lagrini, C. Deslouis, H. Cachet, M. Benlahsen, S. Charvet, Elaboration and electrochemical characterization of nitrogenated amorphous carbon films, Electrochem. Communi. 6 (2004) 245–248.
[29] D. Sopchak, B. Miller, R. Kalish, Y. Avyigal, X. Shi, Dopamine and ascorbate analysis at hydrodynamic electrodes of boron doped diamond and nitrogen incorporated tetrahedral amorphous carbon, Electroanal. 14 (2002) 473–478.
[30] L. Liu, E. Liu, Nitrogenated diamond-like carbon films for metal tracing, Surf. Coat. Tech. 198 (2005) 189–193.
[31] X.Y. Yang, L. Haubold, G. Devivo, G.M. Swain, Electroanalytical performance of nitrogen containing tetrahedral amorphous carbon thin-film electrodes, Anal. Chem. 84 (2012) 6240–6248.
[32] A.C. Ferrari, B. Kleinsorge, G. Adamopoulos, J. Robertson, W.I. Milne, V. Stolojan, L.M. Brown, Determination of bonding in amorphous carbons by electron energy loss spectroscopy, Raman scattering and X-ray reflectivity, J. Non-Cryst. Solids 765 (2000) 266–269.
[33] K.W.R. Gilkes, H.S. Sands, D.N. Batchelder, J. Robertson, W.I. Milne, Direct observation of sp^3 bonding in tetrahedral amorphous carbon using ultraviolet Raman spectroscopy, Appl. Phys. Lett. 70 (1997) 1980–1982.
[34] G. Irmer, A. Dorner-Reisel, Micro-Raman studies on DLC coatings, Adv. Eng. Mater. 7 (2005) 694–705.
[35] P. Merel, M. Tabbal, M. Chaker, S. Moisa, J. Margot, Direct evaluation of the sp^3 content in diamond-like-carbon films by XPS, Appl. Surf. Sci. 136 (1998) 105–110.
[36] T.M. Manhabosco, I.L. Muller, Electrodeposition of diamond-like carbon (DLC) films on Ti, Appl. Surf. Sci. 255 (2009) 4082–4086.
[37] G.M. Fuge, C.J. Rennick, S.R.J. Pearce, P.W. May, M.N.R. Ashfold, Structural characterisation of CN_x thin films deposited by pulsed laser ablation, Diam. Relat. Mater. 12 (2003) 1049–1054.
[38] A. Zeng, E. Liu, S.N. Tan, S. Zhang, J. Gao, Cyclic voltammetry studies of sputtered nitrogen doped diamond-like carbon film electrodes, Electroanal. 14 (2002) 1110–1115.
[39] N.W. Khun, E. Liu, H.W. Guo, Cyclic voltammetric behavior of nitrogen-doped tetrahedral amorphous carbon films deposited by filtered cathodic vacuum arc, Electroanal. 20 (2008) 1851–1856.
[40] Y. Tanakaa, M. Furuta, K. Kuriyama, R. Kuwabara, Y. Katsuki, T. Kondo, Electrochemical properties of N-doped hydrogenated amorphous carbon films fabricated by plasma-enhanced chemical vapor deposition methods, Electrochim. Acta 56 (2011) 1172–1181.
[41] X. Yang, L. Haubold, G. DeVivo, G.M. Swain, Electroanalytical performance of nitrogen-containing tetrahedral amorphous carbon thin-film electrodes, Anal. Chem. 84 (2012) 6240–6248.